VI CONGRESSO NACIONAL DE ENGENHARIA MECÂNICA
VI NATIONAL CONGRESS OF MECHANICAL ENGINEERING
18 a 21 de agosto de 2010 – Campina Grande – Paraíba - Brasil
August 18 – 21, 2010 – Campina Grande – Paraíba – Brazil

THERMAL SIGNATURE MODEL OF A MAIN BATTLE TANK

A. M. Santos, aline@ime.eb.br[1]
R. O. C. Guedes, guedes@ime.eb.br[1]
F. Scofano Neto, scofano@ime.eb.br[1]

[1] Instituto Militar de Engenharia, Seção de Engenharia Mecânica e de Materiais, Praça General Tibúrcio 80, Rio de Janeiro, RJ, 22290-270.

Abstract. *In modern ground warfare, freedom to maneuver undetected around the battlefield is a major factor to determine the outcome of a battle. As infrared (IR) sensors increase in sensitivity, IR signature management becomes ever more necessary for military equipment. Sophisticated thermal signature models are available but are time consuming to run and require detailed input data. In an attempt to provide a first filter of trials data for a high-fidelity computational model and in order to test signature reduction concepts, a simple mathematical formulation is presented in the literature and deals with the generation of a single temperature difference of a ground vehicle for input into a Minimum Resolvable Temperature Difference (MRTD) model. This contribution further extends the accuracy of this approach by incorporating the effects of an orientation factor in the formulation and by employing a MRTD curve from an actual IR camera. This extended procedure is then used in a case study based on the Brazilian Army tank Leopard 1A1 to predict detection range therefore allowing for identification of vehicle surfaces that may require thermal signature reduction. The results here advanced are critically compared with those obtained from the original proposition.*

Keywords*: thermal signature, infrared*

1. INTRODUCTION

The need for thermal signature management has become increasingly important over the past few years due to the advancements in electronics technologies aimed at military sensors. A camouflaged vehicle deemed invisible to the naked eye, but without infrared treatment, once viewed through a thermal sensor, can be easily detected and targeted. As a result, designers realized that the signature aspects of a vehicle should not be left untouched and signature management is becoming more integrated into the concept phase of military ground vehicles. This situation led to the development of highly specialized and often expensive thermal modeling codes like Multi-service Electro-optical Signature Code (MuSES) and Physically Reasonable Infrared Signature Modeler (PRISM) for the prediction of thermal signatures of military ground vehicles. Although extensively used, these high fidelity codes are time consuming and demand detailed input data concerning the vehicle, weather conditions and background scene. In an attempt to provide a first filter of trials data for the more sophisticated software and in order to test signature reducing concepts, Richardson (1998) developed a simple method of generating a single temperature difference of an object which is used as the input data in a minimum resolvable temperature difference (MRTD) model. Richardson and King (2000) employed this technique in a case study based on a contemporary Main Battle Tank (MBT) to predict detection range reduction and thereby identify the areas on the MBT that require thermal signature reduction. Richardson and Coath (2003) extended this model to include low emissivity materials and performed an assessment of the reduction in range associated with the application of low emissivity paints and coatings on a MBT. In this contribution, the accuracy of this model is further extended with the incorporation of the effects of view factors in the formulation and by using an actual MRTD curve furnished by an infrared cameras manufacturer. This extended model is then used in a case study based on one of the Brazilian Army tanks to predict detection range and thermal contrast.

2. MATHEMATICAL MODEL

In this section, the ideas developed by Richardson (1998) are recalled and an extended model is proposed to account for the radiative exchange process among several surfaces comprising a test vehicle.

2.1. Thermal Contrast and Minimum Resolvable Temperature Difference (MRTD)

Thermal signatures almost always result from the difference, or contrast, between the target and its immediate background. Therefore, for an object to be detectable there must be a difference between the radiated energy originating from the object and the radiated energy originating from the background. This thermal contrast can equally be positive, if the object energy is greater than the background energy, or negative. The thermal contrast of an object or target viewed over a band of wavelengths can be described as (Richardson and Coath, 2003; Richardson and King, 2000)

$$C = \frac{\int_{\lambda_1}^{\lambda_2} \varepsilon_{\lambda,\mathrm{TARGET}}\, M_{\lambda,\mathrm{TARGET}}\, d\lambda - \int_{\lambda_1}^{\lambda_2} \varepsilon_{\lambda,\mathrm{BACKGROUND}}\, M_{\lambda,\mathrm{BACKGROUND}}\, d\lambda}{\int_{\lambda_1}^{\lambda_2} \varepsilon_{\lambda,\mathrm{TARGET}}\, M_{\lambda,\mathrm{TARGET}}\, d\lambda + \int_{\lambda_1}^{\lambda_2} \varepsilon_{\lambda,\mathrm{BACKGROUND}}\, M_{\lambda,\mathrm{BACKGROUND}}\, d\lambda} \qquad (1)$$

Where,

ε_λ = spectral emissivity
λ = wavelength of the radiation (μm)

M_λ = spectral radiant blackbody emittance (W m^{-2} μm^{-1}) as given by Planck´s Law = $\dfrac{C_1}{\lambda^5\left[\exp\left(\dfrac{C_2}{\lambda T}\right)-1\right]}$

C_1 = first radiation constant = 3.74 x 10^8 Wm^{-2} μm^4
C_2 = second radiation constant = 1.44 x 10^4 μmK
T = temperature of the object (K)

In an infrared scene, the contrast originated by temperature and emissivity differences between an object and its background provides a figure of merit for the detectability of the target. This detectability depends on the performance of the thermal camera. Among several performance characteristics of a thermal imaging system, the subjective image quality of the camera is measured by its ability to identify temperature differences and spatial details in a scene. These two properties are related to each other and this relation can be expressed by a parameter known as the minimum resolvable temperature difference (MRTD) of the system. MRTD is considered as the most important characteristic of surveillance thermal cameras (Chrzanowski and Park, 2001) and it is measured from a thermal contrast between a uniform background and a standard 4-bar target in the foreground. The MRTD curve shows the dependency of the minimum resolvable temperature on the spatial frequency associated with the bar to bar spacing. Figure 1 shows the MRTD curves for two different thermal imagers (Santos, 2008).

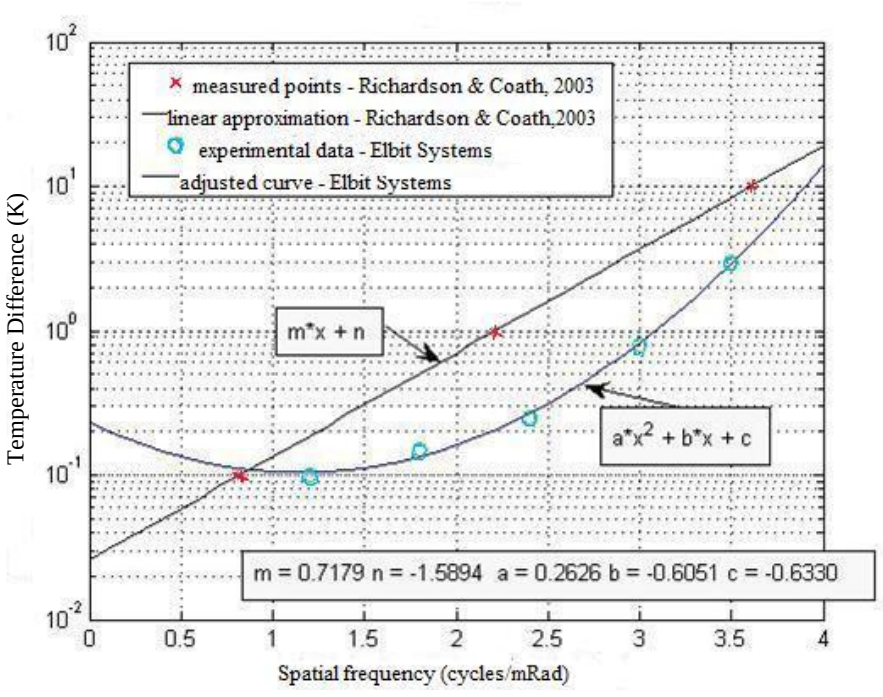

Figure 1. MRTD curve for a laboratory thermal imager (Richardson and Coath, 2003) and for a typical thermal imaging camera manufactured by Elbit Systems Ltd. (Santos, 2008)

2.2 Single Temperature Difference Model

The technique described by Richardson (1998) is now employed to generate a single temperature difference for a Main Battle Tank. In summary, this technique considers the target to be composed of several areas each of them with a different temperature and emissivity. The total power emitted from the target over the waveband of interest is given by

$$P_{TARGET} = \sum_i P^i{}_{TARGET} = \sum_i M^i{}_{TARGET}\ A^i{}_{TARGET} \tag{2}$$

Where $A^i{}_{TARGET}$ is the area of the i^{th} element and M^i is the total radiant emittance of the i^{th} element integrated over the waveband of interest. Similarly, the background immediately adjacent to the target is considered to be composed of many areas obeying the following relation

$$A = \sum_i A^i{}_{TARGET} = \sum_j A^j{}_{BACKGROUND} \tag{3}$$

The total power emitted from the background can be calculated in the same manner as in Eq. (2). Therefore, the difference between the target and background power is written as

$$\Delta P = P_{TARGET} - P_{BACKGROUND} \tag{4}$$

The difference power ΔP is then used to obtain the equivalent difference temperature referenced to standard laboratory temperature of 293 K such that

$$\int_{\lambda_1}^{\lambda_2} M_\lambda (293+\Delta T, \varepsilon = 1)\ d\lambda = \frac{P' + \Delta P}{A} \tag{5}$$

Where P´ is the power emitted by a blackbody ($\varepsilon = 1$) target of area A at 293 K. Solving Eq. (5) for ΔT provides the input values for range calculations based on the Johnson criteria for detection, recognition and identification. The spatial frequency is related to the Johnson criteria and critical spatial dimension of the target by

$$x = \frac{NR}{H} \tag{6}$$

where:
x = spatial frequency (cycles/mRad)
N = number of resolvable cycles for detection, recognition or identification (Table 1)
R = range to target (km)
H = critical target dimension (m)

Table 1. The Johnson Criteria (Johnson, 1958)

Criterion	Number of Resolvable Cycles (N)
Detection	1.0 ± 0.25
Recognition	4.0 ± 0.8
Identification	6.4 ± 1.5

On the other hand, the atmospheric effects are approximated by a Beer´s Law estimate as

$$\Delta T_R = \Delta T \exp(-\varphi R) \tag{7}$$

where φ is the atmospheric attenuation coefficient. According to Fig. (1), the MRTD is assumed to be log-linear and therefore is represented by (Richardson and Coath, 2003; Richardson and King, 2000)

$$\log(\Delta T_R) = m x + n \tag{8}$$

where m and n are characteristics of the MRTD curve. Upon combination of Eq. (7) and Eq. (8) it is then possible to derive an expression for range thus

$$R = \frac{H(\ln(\Delta T) + \ln(10)n)}{\ln(10)mN + \varphi H} \tag{9}$$

where ln(10) accounts for the conversion between base 10 and natural logarithms.

Now, computational methods can be used to produce a single detection, recognition or identification range for a complex object given the power and the size of the individual radiating elements making up the object.

This model has been verified by several field trials against standard painted vehicles ($\varepsilon \approx 1$) and the agreement between the modeled ranges for identification, recognition and identification and their measured counterparts was excellent (Richardson and Coath, 2003).

2.3 Extension of the model

The model originally proposed by Richardson (1998) described above was extended by Richardson and Coath (2003) to include low emissivity materials since, as the emissivity of a material is reduced, its corresponding reflexivity increases. Therefore, the model was modified to include a reflection component as follows:

$$M^{i}_{TARGET} = \int_{\lambda_1}^{\lambda_2} \frac{\varepsilon_{\lambda,TARGET}\, C_1}{\lambda^5[\exp\left(\frac{C_2}{\lambda T_{TARGET}}\right) - 1]}\, d\lambda + \int_{\lambda_1}^{\lambda_2} \frac{(1-\varepsilon_{\lambda,TARGET})\, C_1}{\lambda^5[\exp\left(\frac{C_2}{\lambda T'_{BACKGROUND}}\right) - 1]}\, d\lambda \tag{10}$$

$$M^{i}_{BACKGROUND} = \int_{\lambda_1}^{\lambda_2} \frac{\varepsilon_{\lambda,TARGET}\, C_1}{\lambda^5[\exp\left(\frac{C_2}{\lambda T_{BACKGROUND}}\right) - 1]}\, d\lambda + \int_{\lambda_1}^{\lambda_2} \frac{(1-\varepsilon_{\lambda,TARGET})\, C_1}{\lambda^5[\exp\left(\frac{C_2}{\lambda T_{TARGET}}\right) - 1]}\, d\lambda + \int_{\lambda_1}^{\lambda_2} \frac{(1-\varepsilon_{\lambda,TARGET})\, C_1}{\lambda^5[\exp\left(\frac{C_2}{\lambda T'_{BACKGROUND}}\right) - 1]}\, d\lambda \tag{11}$$

where, $T'_{BACKGROUND}$ is the radiometric temperature of the reflected background scene (typically, the sky) and $T_{BACKGROUND}$ is the temperature of the immediately adjacent surface.

In this contribution, the ideas summarized above are further extended in the following manner: First, an alternative MRTD curve is derived based on data furnished by thermal cameras manufacturer Elbit Systems Ltd (Santos, 2008). Instead of the linear approximation adopted by Richardson and King (2000), the Minimum Squares Method is employed to fit the data provided by Elbit Systems (Fig. (1)) to a parabola of the form

$$\log(\Delta T_R) = a\,x^2 + bx + c \tag{12}$$

Then, following the methodology developed by Richardson (1998), the corresponding expression for the determination of the range is derived as

$$a\,N^2 \ln(10)\,R^2 + (b\,H\,N\ln(10) + H^2\,\varphi)\,R + H^2(c\ln(10) - \ln(\Delta T)) = 0 \tag{13}$$

Moreover, the effects of the radiative exchange process among the several surfaces that comprises the vehicle are taken into account, and therefore the total radiative energy leaving a surface is written in terms of its radiosity J rather than its emittance M. Thus, in addition to considering that the i^{th} element emits thermal radiation as a function of its temperature and reflects the energy that comes from the background scene only as in Eq. (10) (Richardson and Coath , 2003), this contribution also considers the energy coming from all other parts of the vehicle that is reflected by the i^{th} element. In order to accomplish this task, the model due to Richardson and Coath (2003) is modified to adhere to the ideas brought up by Ozisik (1973) for the simplified zone analysis of radiative exchange in enclosures as follows:

The enclosure is assumed to be composed of a finite number (NS) of surfaces so that the radiative properties, the temperature, and the intensity of radiation leaving the surfaces are uniform and independent of direction over the surface of each zone. Temperature is prescribed in each zone. These assumptions imply also that the surfaces are diffuse

emitters and diffuse reflectors. An additional condition is that the surfaces are opaque. When these assumptions are applied, the expression for the spectral radiosity J_λ of the i th surface (i.e., the radiant energy leaving the surface) simplifies to

$$J_{\lambda,i} = \varepsilon_{\lambda,i}\pi I_{\lambda,blackbody}(T_i) + \rho_{\lambda,i}\sum_{j=1}^{NS} J_{\lambda,j}F_{i-j} \tag{14}$$

where,

$\rho_{\lambda,i}$ = spectral hemispherical reflexivity for the i th surface

F_{i-j} = diffuse view factor between surfaces i and j

$I_{\lambda,blackbody}$ = spectral radiation intensity for a blackbody = $\dfrac{C_1/\pi}{\lambda^5\left[\exp\left(\dfrac{C_2}{\lambda T}\right)-1\right]}$

And for the case of gray surfaces Eq. (14) becomes

$$J_i = \varepsilon_i\pi I_{blackbody}(T_i) + (1-\varepsilon_i)\sum_{j=1}^{NS} J_j F_{i-j} \tag{15}$$

3. MODEL IMPLEMENTATION AND RESULTS

Field trials were conducted for a Leopard 1 A1 Tank from the Brazilian Army in March and April, 2007. The vehicle was divided in 27 surfaces and temperature readings for each surface were taken with infrared thermometer model Minipa MT-350 (range -30°C to 550°C with a precision of ±2°C from -30°C to 100°C and ±2% from 101°C to 550°C). The tests were performed for several combinations of weather and vehicle conditions, namely, vehicle under the sun, in shade or at night, vehicle in motion or not and engine running with vehicle stationary or not. The selected surfaces, its areas and the mean surface temperatures for a typical test performed are shown in Fig. (2). Atmospheric attenuation coefficient was supposed to vary according to weather conditions from 0.2 (clear) to 1.0 (cloudy). For partially cloudy skies the value 0.6 was chosen and for trials at night this value was set at 0.4.

For the case of the extended model with view factors here advanced, Eq. (15) for NS = 27 was rewritten as

$$\sum_{j=1}^{27}\left[\frac{\delta_{ij} - (1-\varepsilon_i)F_{i-j}}{\varepsilon_i}\right] J_j = \pi I_{blackbody}(T_i) \tag{16}$$

where δ_{ij} is the Kronecker delta. Equation (16) may be written in matrix form as

$$[K]\{J\} = \{I\} \tag{17}$$

where [K] is the coefficients matrix bearing information on emissivities and view factors among the surfaces, {J} is the vector of unknown radiosities and {I} the vector describing the blackbody radiative intensity for each surface as a function of its known temperature. Upon determination of the unknown radiosities J, the Newton-Raphson method was employed to solve Eq. (5) for ΔT with M replaced by J, since the extended model then considered the view factors among the surfaces. The resulting ΔT, the selected Johnson criterion N and a critical target dimension H were then used as an input in Eq. (9) or Eq. (13) depending on the MRTD curve adopted. The corresponding range R was thus obtained.

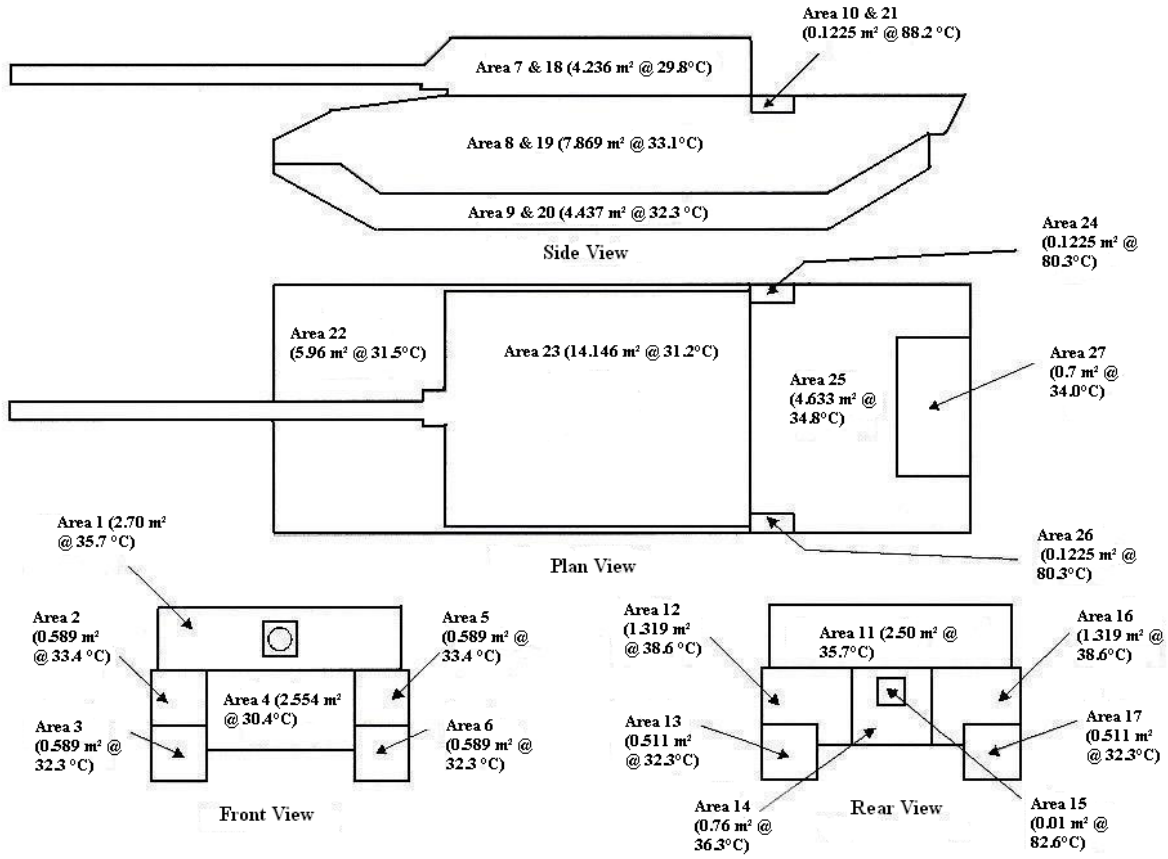

Figure 2. Temperature survey of Brazilian Army´s Leopard 1 A1 Battle Tank (A. M. Santos, 2008). Test conditions: sunny day, ambient temperature of 34 °C, vehicle stationary at shade conditions with engine running.

Figure 3 shows the variation of the detection range in kilometers with emissivity (Johnson criterion N = 1) for the model due to Richardson and Coath (2003), Eqs. (2) – (11), for the situation of both MRTD curves presented here (Eq. (8) - linear and Eq. (12) – parabolic). The vehicle is stationary at shade conditions with its engine running at an ambient temperature of 34°C in a sunny, bright day. The range for detection of side, front, rear and top surfaces of the vehicle is depicted. Clearly, the detection range for all surfaces is greater for the parabolic MRTD curve than for the linear one. This means that a thermal imager that follows the parabolic curve detects the vehicle within a greater distance than the one that follows the linear approximated curve. Therefore, with respect to this variable, the thermal imager originally studied by Richardson and Coath (2003) underestimates the detection range for the battle tank. As far as emissivity is concerned, it is noticed that as emissivity increases, the detection range significantly decreases and therefore surfaces coated with highly emissive paints help to reduce the thermal signature of the vehicle.

Figure 4 shows the results for the contrast under the same conditions of Fig. (3). Since contrast depends essentially on temperature and emissivity, different MRTD curves furnishes the same contrast for a certain surface with a fixed emissivity, as apparent from Fig. (4). It is also observed on Fig. (4) that contrast decreases with increasing emissivities except for the small rage regarding $\varepsilon = 0.9$ to $\varepsilon = 1$. As the target emissivity approaches $\varepsilon = 1$ (blackbody behavior), Eq. (1) reveals that the contrast may increase after attaining a lower bound depending on the temperature difference between the chosen surface and the background. This behavior is observed in a lesser degree on Fig. (5) where test conditions are such that the engine is not operating and therefore the average surface temperatures are very close to those on the background. It should also be mentioned that all other tests conducted for different weather and vehicle conditions revealed the same trends presented in Fig. (3) and Fig. (4).

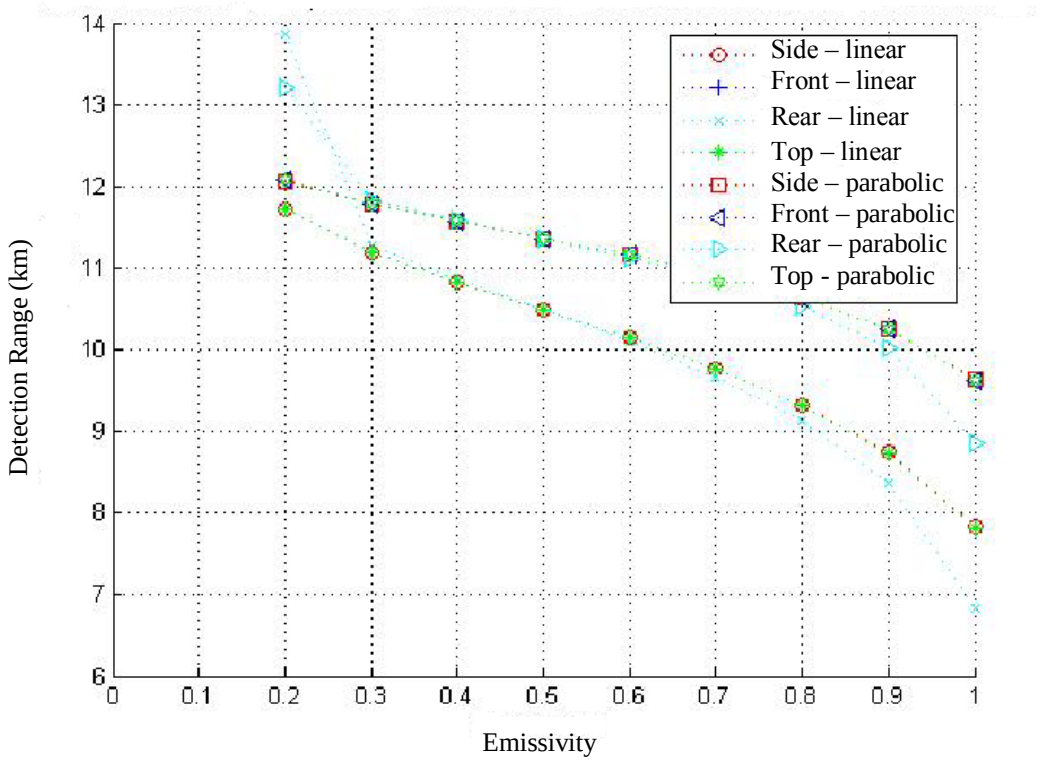

Figure 3. Variation of detection range with emissivity for two MRTD curves of different shape when considering the extended model by Richardson and Coath (2003). Test conditions: sunny day, ambient temperature of 34 °C, vehicle stationary at shade conditions with engine running.

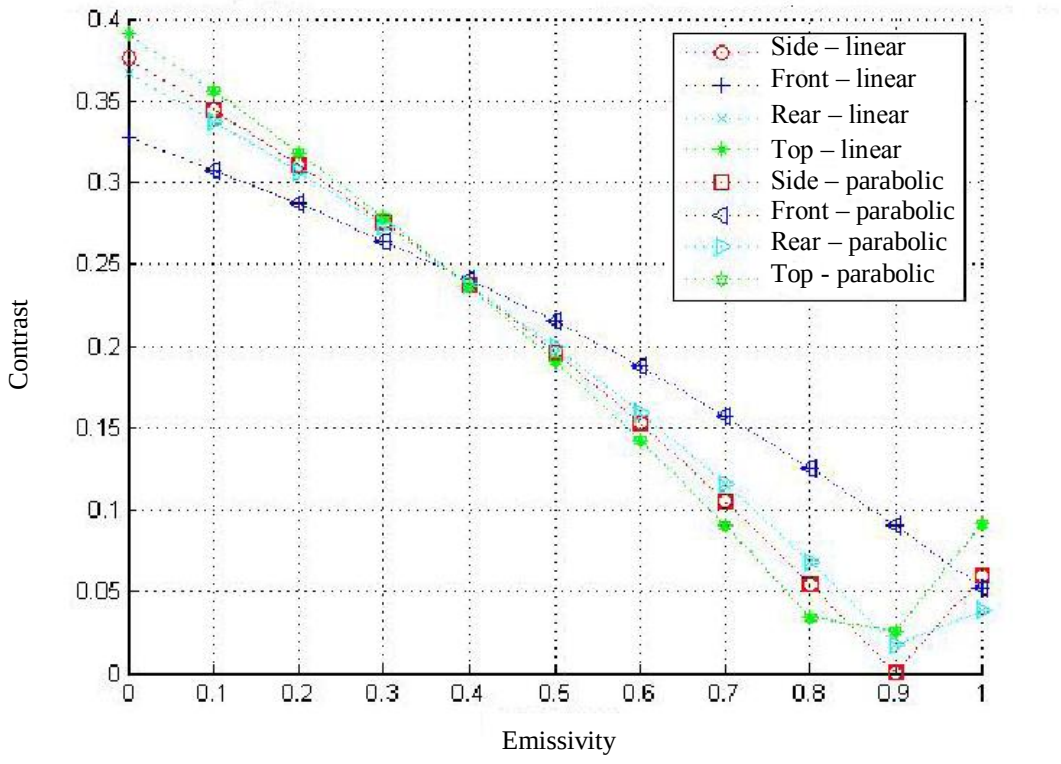

Figure 4. Variation of thermal contrast with emissivity for two MRTD curves of different shape when considering the extended model by Richardson and Coath (2003). Test conditions: sunny day, ambient temperature of 34 °C, vehicle stationary at shade conditions with engine running.

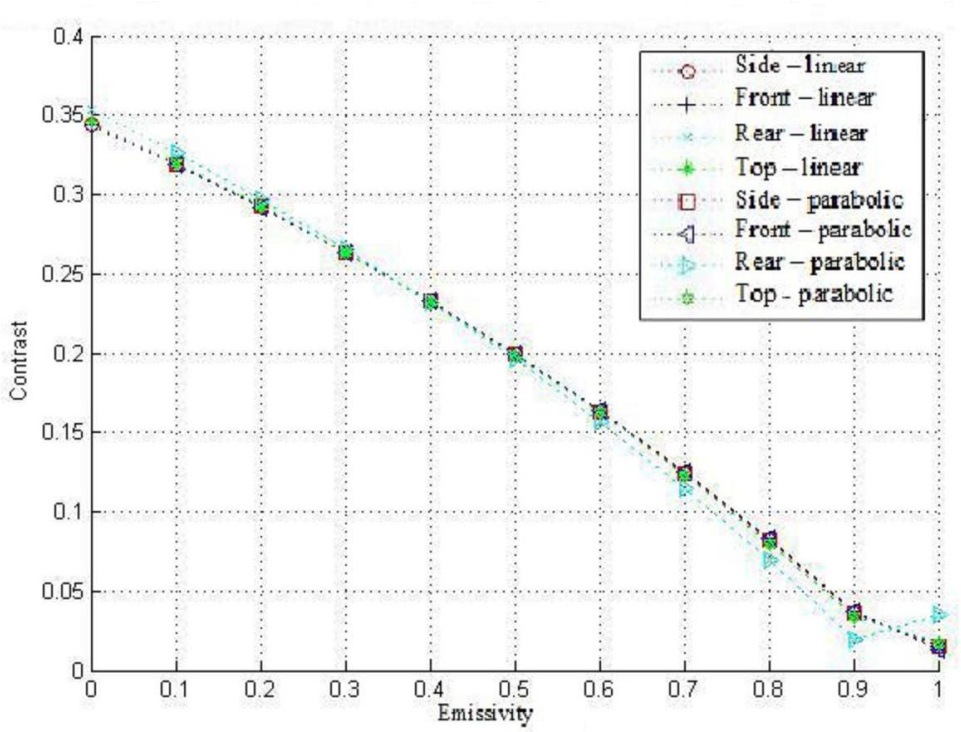

Figure 5. Variation of thermal contrast with emissivity for two MRTD curves of different shape when considering the extended model by Richardson and Coath (2003). Test conditions: cloudy sky, ambient temperature of 29 °C, vehicle stationary on open field with engine not running.

Next, results for the extended model due to Richardson and Coath (2003), Eqs. (2) – (11), and for the extended model modified here with the inclusion of view factors, Eqs. (12) – (17), are compared for the situation of the parabolic shaped MRTD curve only.

Figures 6 and 7 show, respectively, the detection range and the contrast as a function of emissivity for side, rear, front and top surfaces of the vehicle. The test conditions depicted are the same of the previous discussion. As it can be observed in Fig. (6), all results for detection range for the corrected model, i.e., when the analysis includes the exchanges among the various surfaces, fall below the curves for their counterparts analyzed with the uncorrected model, i.e., the one that considers reflection from the adjacent background only. So, the combined effects of emission and reflection overestimates the detection range when analyzed with the model due to Richardson and Coath (2003). For instance, in the case of $\varepsilon = 0.5$, the model due to Richard and Coates (2003) predicts a detection range of roughly 12 km for the top surface of the vehicle. In reality, the present model indicates that the actual range is approximately 8.5 km for this situation, suggesting that the combatant should come closer (3.5 km) to the target in order to detect it. In addition, the curves for the corrected model are much less steep than the ones for the uncorrected model. When the corrected model is employed, results for side and top surfaces become practically independent of emissivity whereas results for rear and front surfaces follow the trends for the uncorrected model. This is due to the orientation of each surface in relation to the other ones which ultimately determines the amount of energy being reflected or not. Rear and front surfaces of the vehicle are less influenced by the view factors of the other surfaces and therefore the two models furnish similar results in this case.

As for the contrast, since ambient temperature is close to the mean temperature of most of the surfaces for this test conditions, results show a low contrast for both models.

As far as the precision of ±2°C in the thermometer readings is concerned, it should be mentioned that according to Santos (2008), the detection range evaluated by this methodology presents a maximum deviation of ±200 m. When this precision range is taken into account in the contrast calculation, results indicate a maximum deviation of ± 0.005. Therefore, it can be affirmed with confidence that the influence of measurement readings is not too relevant within the context of this research.

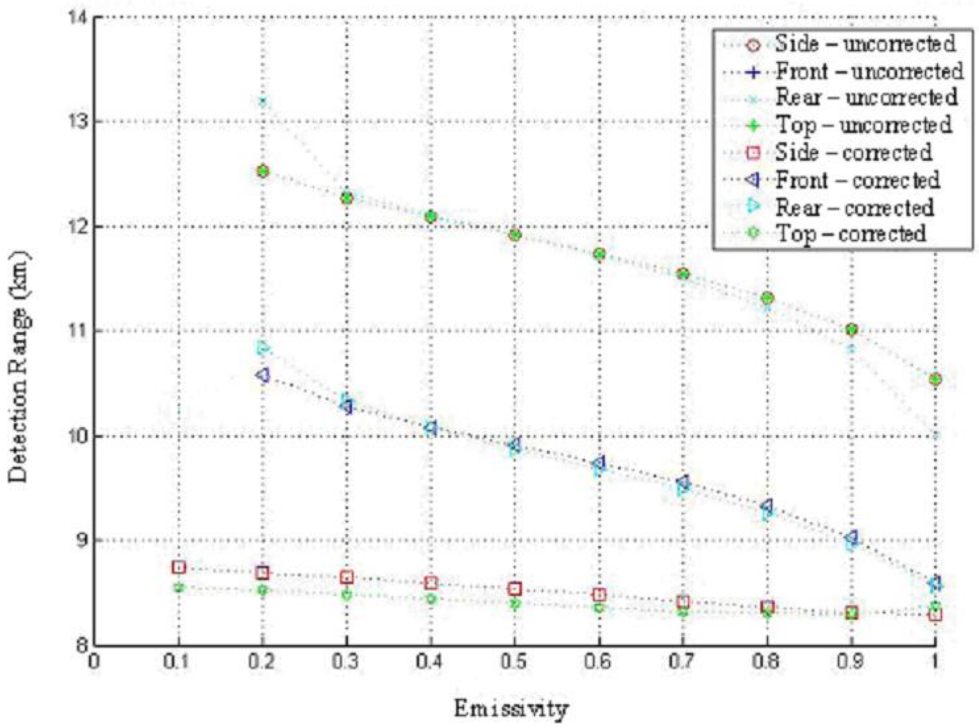

Figure 6. Variation of detection range with emissivity for parabolic shaped MRTD curve when considering the extended model with and without view factor correction. Test conditions: sunny day, ambient temperature of 34 °C, vehicle stationary at shade conditions with engine running.

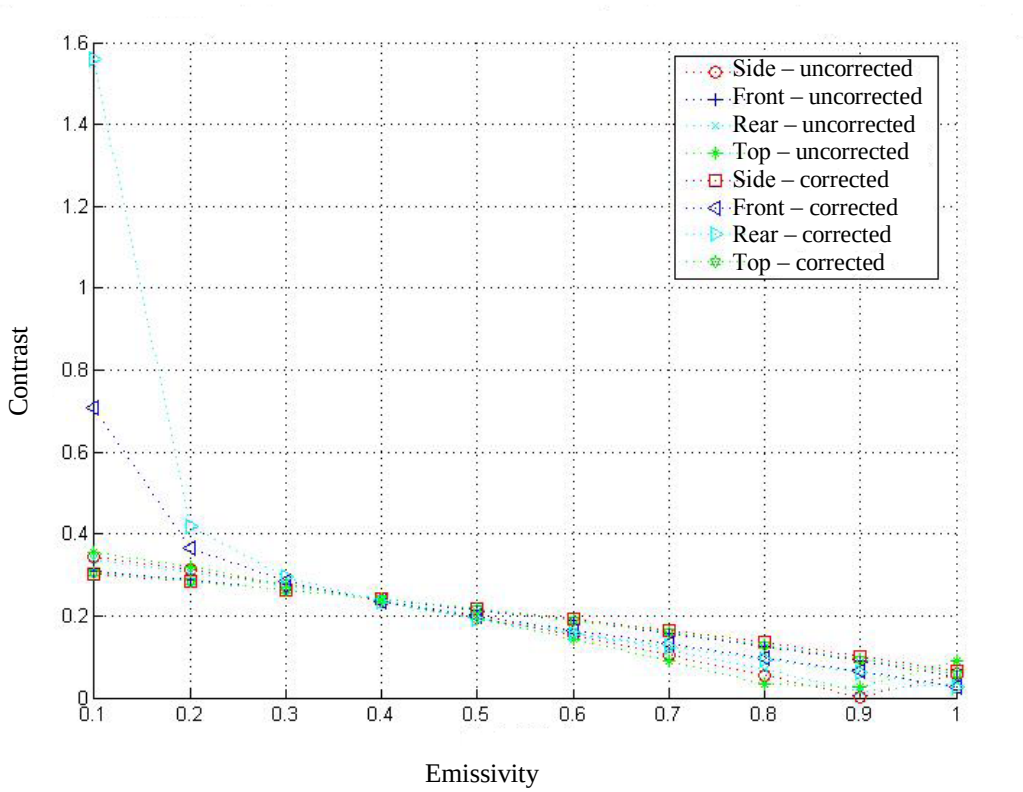

Figure 7. Variation of thermal contrast with emissivity for parabolic shaped MRTD curve when considering the extended model with and without view factor correction. Test conditions: sunny day, ambient temperature of 34 °C, vehicle stationary at shade conditions with engine running.

In conclusion, this paper has advanced a simple yet effective model to evaluate the thermal signature based on the ideas of Richardson (1998) but including the radiative heat transfer that takes place among the several surfaces of an armored vehicle. This model was tested on a Leopard 1 A1 tank and the basic conclusion drawn is that, in comparison to this research, the modification proposed by Richardson and Coath (2003) underestimates the detection range of the vehicle when employing their original sensor whereas it overestimates this particular range when employing a different sensor. As a final note, it should be mentioned that the ideas discussed in this contribution are the early stages of an on-going research that aims to develop models for the management of infrared signature of ground vehicles currently in use by the Brazilian Army.

4. ACKNOWLEDGEMENTS

The authors are indebted to Elbit Systems Ltd. for kindly providing information on thermal imagers and to the Parque Regional de Manutenção da 1ª Região Militar (PqRMnt/1) of the Brazilian Army for making available the main battle tank Leopard 1 A1 nicknamed “Papagaio” for the field tests conducted in March – April 2007.

5. REFERENCES

Chrzanowski, K., and Park, S. N., 2001,”Evaluation of Thermal Cameras for Non-Destructive Thermal Testing Applications”, Infrared Physics & Technology, vol.42, No. 2, pp. 101-105.

Johnson, J., 1958, “Analysis of Image Forming Systems,” in Proceedings of Image Intensifier Symposium, Warfare Electrical Engineering Department, U.S. Army Research and Development Laboratories, Ft. Belvoir, pp. 244–273.

Ozisik, M. N., 1973, “Radiative Transfer and Interactions with Conduction and Convection”, Wiley-Interscience.

Richardson and Coath, 2003,”Low Resolution Signature Modelling of a Main Battle Tank”, in Targets and Backgrounds IX: Characterization and Representation, Wendell R. Watkins, Dieter Clement, William R. Reynolds, Editors, Proceedings of SPIE, vol. 5075, pp. 28-38.

Richardson, M. A., and King, S. J., 2000,”Modelling the Signature Vulnerability of a Main Battle Tank”, Journal of Battlefield Technology, vol. 3, No. 3, pp. 29-34.

Richardson, M. A., 1998,”Reducing Complex Infra-red Scenes to a Single Temperature Difference”, Journal of Defence Science, vol. 3, No. 3, pp. 397-403.

Santos, A. M., 2008, “Thermal Signature Modelling of a Battle Tank” (in Portuguese), M. Sc. Dissertation, Instituto Militar de Engenharia, Rio de Janeiro, Brazil.

6. RESPONSIBILITY NOTICE

The authors are the only responsible for the printed material included in this paper.